Journal of the Korea Academia-Industrial cooperation Society
Vol. 21, No. 9 pp. 405-413, 2020

https://doi.org/10.5762/KAIS.2020.21.9.405
ISSN 1975-4701 / eISSN 2288-4688

Modeling on Rheological Behavior of Cement Paste under Squeeze Flow

Byeong-Hyeon Min
Division of Mechanical, Automobile, Robot Component Engineering, Dong-eui University

압축 유동하에 있는 시멘트 페이스트의 유변학적 거동에 관한 모델링

민병현
동의대학교 기계자동차로봇부품공학부

Abstract The normal stress of cement paste measured under squeeze flow is divided into an elastic solid region at strains between 0.0003 and 0.003 and a strain-hardening region at strains of 0.003 and 0.8. A modeling equation at the strain-hardening region was proposed. First, from the viewpoint of fluid behavior, the power-law non-Newtonian fluid model, with a power-law consistency (m) of 700 and a power index (n) of 0.2, was applied. The results showed good agreement with the experimental results except for an elastic solid region. Second, from the viewpoint of ductile yielding solid behavior, the force balance model was applied, and the friction coefficient between the sensor part measuring the load and the surface of the cement paste was derived as a polynomial of the normal strain by applying the half-interval search method to the experimental data. The results showed good agreement with the experimental results only in the middle normal strain region at strains between 0.003 and 0.3. The rheological behavior of the cement paste under squeeze flow was more consistent with the experimental results from the viewpoint of power-law non-Newtonian fluid behavior than from the viewpoint of ductile yielding solid behavior in the strain-hardening region.

요 약 압축 유동하에서 측정된 시멘트 페이스트의 수직 응력은 변형률의 증가에 따라 변형률이 0.0003에서 0.003 사이 구간인 탄성 고체 구간과 변형률이 0.003에서 0.8 사이 구간인 변형률 경화 구간으로 나누어진다. 두 구간 중 변형률 경화 영역에서 유변학적 특성을 분석하기 위해 모델링 식이 제안되었다. 첫째, 유체 거동의 관점에서, 지수법칙 일관성 지수 m=700 및 멱지수 n=0.2를 갖는 지수법칙 비뉴토니언 모델이 적용되었다. 적용 결과는 탄성 고체 구간을 제외하고는 실험 결과와 좋은 일치를 보여주었다. 둘째, 연성 고체 거동의 관점에서 힘 평형 모델이 적용되었으며, 하중을 측정하는 센서부와 시멘트 페이스트 표면 간의 마찰 계수가 실험데이터에 반구간탐색법을 적용하여 변형률의 다항식으로 도출되었다. 적용 결과는 변형률이 0.003에서 0.3 사이 구간인 중간 영역에서만 실험 결과와 좋은 일치를 보여주었다. 따라서, 압축 유동 하의 시멘트 페이스트의 유변학적 거동은 변형률 경화 구간에서 연성 고체 거동의 관점보다는 지수법칙 비뉴토니언 유체 거동의 관점에서 실험 결과와 더 일치함을 보여주었다.

Keywords : Rheology, Power-Law Model, Force Balance Model, Squeeze Flow, Cement Paste

This Work was supported by Dong-eui University Foundation Grant(2017).
*Corresponding Author : Byeong-Hyeon Min(Dong-eui Univ.)
email: bhmin@deu.ac.kr
Received June 8, 2020 Revised August 28, 2020
Accepted September 4, 2020 Published September 30, 2020

1. Introduction

The rheology of cement paste is complex and flow properties, such as the relationship between shear rate and viscosity, are the subject on for going research[1]. Flow properties incorporate strain rate and time dependent behavior under large deformation. Typically, result shows that cement paste obeys a Bingham type of behavior. A connection is made to microstructure in that the flocculated system yields or breaks down in the small strain region[2-4]. Although only shear flows have been emphasized in the rheological research of cement paste[5-9], there is another class of flow known as shear free flow, that includes elongation, squeeze and planar flows, which are important to compression processing[10-13]. It is a dominant factor when considering processes such as mixing, compression processing, extrusion and 3D printing processing[14-18]. Squeeze flow experiments have not been applied extensively to cement paste because of the difficulties involved in generating squeeze flow in a controlled experiment. These points mean that the rheological characteristics of cement paste have not been completely analyzed. Squeeze test can also be extended to investigate mortar and concrete because of size not possible in shear flow. Cement paste is investigated as a first step.

So far, rheological models for cement paste have been mainly concentrated on predicting the flow behavior of fresh cement paste described by the relationship between shear stress and shear rate using mathematical equations which were obtained curve-fitting experimental results[19-22]. These rheological behavior of fresh cement paste were specified by flow characteristics at large strain region made under a small shear rate.

In this paper, rheological behavior of fresh cement paste under squeeze flow is suggested by modeling the relationship between normal stress and normal strain of fresh cement paste from non-Newtonian fluid and ductile yielding solid deformation points of view. The normal stresses of the cement paste measured under compression behavior are divided into an elastic solid region at the strain between 0.0003 and 0.003 and a strain hardening region at the strain between 0.003 and 0.8 according to the increase of the strain. Power-law fluid model is considered for non-Newtonian fluid behavior based on the simulation results of squeezing flow[23-25] and the force balance analysis is applied for ductile yielding solid behavior based on the simulation of metal forming[26]. In order to better simulate the measured normal stress with the power-law fluid model, the geometric factor of cement paste(CGF) obtained from the experimental results is considered. The consistency m of 700 and the power index n of 0.2 in power-law fluid model are obtained by a trial and error method. Experimental conditions for the application of numerical analysis by the Newton-Raphson method are the initial sample height of 18 mm and the squeeze motion amplitude of 10 mm.

In dealing with a force balance analysis the following pertinent assumptions are invoked[26]. The direction of the load defines principal direction, and principal stresses do not vary on planes. The model result reflects the measurement result well by applying the friction coefficient formula(expressed in polynomial) obtained by applying the measurement result of the normal stress to the friction coefficient included in the analysis formula. The friction coefficient between the upper plate of the experiment system and the sample surface is derived by applying the half-interval search method so that the measured normal stress value is similar to the force balance simulation analysis value, and is expressed from the strain polynomial.

From two kinds of model results, it is shown

that the rheological behavior of the cement paste in the strain hardening region at the strain between 0.003 and 0.8 where the normal strain under squeeze motion is large is more consistent with the experimental results in terms of non-Newtonian fluid behavior with CGF than in terms of ductile yielding solid behavior.

2. Experiment

2.1 Experimental procedure and system

The apparatus consists of a top platen connected to a load cell, and a bottom container as shown in Fig. 1. The diameter of a top plate is 203.2 mm, and the diameter of a bottom container to keep cement paste is 360 mm. Initial sample heights are 18 and 36 mm. The experimental time is 120 seconds. The load and displacement of the sample are measured with a load cell and a linear variable differential transformer (LVDT). The load cell measured only the normal component of the load, and the average normal stress is obtained by dividing the load by the area of the top plate. The capacity of the load cell is 1000 N[10].

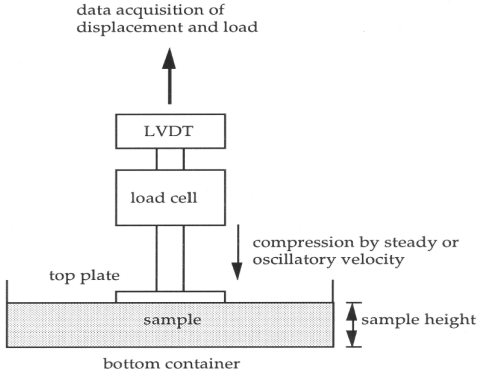

Fig. 1. Schematic diagram of squeeze flow experimental system

2.2 Logarithmic normal strain under constant squeezing velocity

Squeeze flow experiment is performed under constant squeezing velocity because of its easy control. The normal strain and strain rate are as follow:

$$\epsilon(t) = \ln\left(\frac{h(t)}{h_o}\right) = \ln\frac{(h_o - d_o(t))}{h_o} \quad (1)$$

$$\epsilon(\dot{t}) = \frac{d\epsilon}{dt} = \frac{\dot{h}}{h(t)} \quad (2)$$

where, h is a sample height, d_o is an amplitude of ramp signal and h_o is an initial sample height, and $\dot{h}$ is a constant velocity. Table 1. shows the experimental condition for constant velocity squeeze flow experiment[10]. The average normal strain rates are obtained by the arithmetic mean of initial and final strain rates since its values increase logarithmically with squeeze motion of sample as expressed by Eq. (2). However, there was not much difference between initial and final normal strain rates except a larger amplitude of squeeze motion like 10mm.

Table 1. Experimental conditions of constant velocity squeeze experiments

Initial sample height(mm)	Amplitude of squeeze motion(mm)	Velocity (mm/s)	Average strain rate(s^{-1})
36	1	0.00833	0.000235
	5	0.04167	0.001251
18	1	0.00833	0.000476
	5	0.04167	0.002760
	10	0.08333	0.007523

3. Model on rheological behavior under squeeze motion

3.1 Model of fresh cement paste as a power-law fluid at large strain region

Fresh cement paste is considered as a non-Newtonian fluid since its viscosity is a function of strain rate like the power-law fluid, such as $\eta(\dot{\gamma}) = m\dot{\gamma}^{n-1}$, η is an apparent viscosity, $\dot{\gamma}$ is a shear rate[1]. Here, m and the dimensionless

n are parameters commonly called the consistency and power-law index, respectively. The squeeze flow problem for a power-law fluid has been solved by Leider and Bird[21]. Cylindrical coordinates, taking $v_r=v_r(r,z)$, $v_z=v_z(z)$, and $p=p(r)$, the quasi-steady state assumption, no-slip condition between cement paste and sensor and disregarding all inertial terms, are considered. In the light of these simplifying assumptions, the pressure profile is calculated by applying the continuity and momentum equations:

$$P = P_a + m\frac{(2+s)^n}{2^n(n+1)}\frac{(-\dot{h})^n R^{(1+n)}}{h^{(1+2n)}}[1-(\frac{r}{R})^{1+n}] \quad (3)$$

where s=1/n, h is the sample height, $\dot{h}=\frac{dh}{dt}$ is the squeeze velocity, R is the radius of sample. The instantaneous force(F_N) at z=h is obtained by integrating pressure profile over the disk surface:

$$F_N = m\pi\frac{(2+s)^n}{2^n(3+n)}\frac{(-\dot{h})^n R^{3+n}}{h^{1+2n}} \quad (4)$$

The average normal stress(σ_m) at disk is calculated:

$$\sigma_m = \frac{F_N}{\pi R^2} = m\frac{(2+s)^n}{2^n(3+n)}\frac{(-\dot{h})^n R^{1+n}}{h^{1+2n}} \quad (5)$$

Eq. (5) is expressed by invoking the definition of logarithmic strain rate:

$$\sigma_m = m\dot{\epsilon}^n\frac{(2+s)^n}{2^n(3+n)}(\frac{R}{h})^{1+n} \quad (6)$$

where $\dot{\epsilon}=-\frac{\dot{h}}{h}$. The radius of sample(R) is assumed as constant because it is prevented from increasing due to a surrounded sample around plate. The parameters m and n are obtained by a trial and error method from Eq. (6) as 700 and 0.2, respectively. Experimental conditions for the application of numerical analysis by the Newton-Raphson method were the initial sample height of 18 mm and the squeeze motion amplitude of 10 mm.

From Eq. (6), a geometric factor of power law fluids(PGF) which shows the effect of the dimensionless geometric parameter, R/h, in squeeze flow can be defined:

$$PGF = (\frac{R}{h})^{1+n} \quad (7)$$

Fig. 2. shows the comparison of measured and calculated normal stresses after applying m and n values into Eq. (6) based on the power-law fluid model of cement paste. The measured normal stress of the cement paste with increasing normal strain under squeeze motion is divided into three stages with a "S" shape such as a linear region between 0.0003 and 0.003 defined as stage I, a steady increase region between 0.003 and 0.3 defined as stage II, and a rapid increase region between 0.3 and 0.8 defined as stage III. In this paper, Stage I is defined as an elastic linear region and stage II and III are integrated as strain hardening region. Experimental model equations that can predict the normal stress measured in the strain hardening region are proposed. As shown in Fig. 2, the power-law fluid model applying PGF hardly reflects the experimental results in stages I and II, and is in good agreement with the experimental results only in stage III. From the analysis of measured normal stress, a stage I at small strain region shows an elastic solid behavior of cement paste and stage II & III at large strain region shows a strain hardening behavior of cement paste.

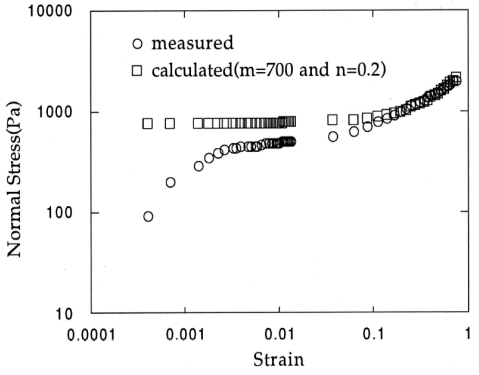

Fig. 2. Comparison of measured and calculated normal stresses based on power law fluid model(Initial sample height: 18mm, Average strain rate: 0.007523s^{-1})

There is a deviation between measured and calculated normal stresses both at small strain region between 0.001 and 0.003 and at middle strain region between 0.003 and 0.3 though it shows good agreement at large strain region between 0.3 and 0.8. This discrepancy seems due to a different geometry factor between power-law fluid and fresh cement paste. Fresh cement paste has a different geometry factor from power-law fluid.

The ratio of the measured normal stress(σ_m) and the terms excluding PGF in Eq. (6), $\frac{\sigma_m}{[m\dot{\epsilon}^n \frac{(2+s)^n}{2^n(3+n)}]}$ is expressed as a function of (R/h) as shown in Fig. 3. The CGF is imposed by a polynomial function of (R/h):

$$CGF = \sum_{i=0}^{k} a_i \left(\frac{R}{h}\right)^i \quad (8)$$

where i includes the parameters n, a_i are obtained from the curve fitting method, and k is taken as 3rd order in this experiment. The model of normal stress(σ_{cal}) reflecting CGF is:

$$\sigma_{cal} = m\dot{\epsilon}\frac{(2+s)^n}{2^n(3+n)}\left[0.061\left(\frac{R}{h}\right)^3 - 1.87\left(\frac{R}{h}\right)^2 + 2.3\left(\frac{R}{h}\right) - 61.15\right] \quad (9)$$

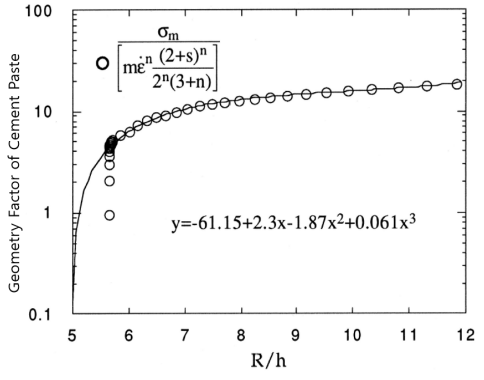

Fig. 3. Geometry factor of cement paste based on experimental result(m=700, n=0.2)

Fig. 4. shows the contribution of PGF and CGF. The power-law fluid model result reflecting PGF factor shows agreement with the experimental results only in the region of large normal strain between 0.3 and 0.8. The power-law fluid model result reflecting the CGF factor shows good agreement compared with the measured normal stress at large strain region between 0.003 and 0.8 because the CGF factor is derived from experimental results. This means that the fresh cement paste follows the power law fluid behavior at large strain region.

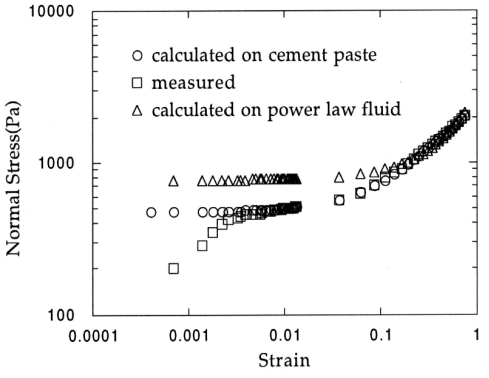

Fig. 4. Effect of the geometry factor on normal stress (Initial sample height: 18mm, Average strain rate: 0.007523s^{-1}, m=700, n=0.2)

Fig. 5. shows the comparison of measured and modeled normal stresses based on the geometry factor of cement paste for various average strain rates with the sample height of 18mm. In spite of various average strain rates, the modeled normal

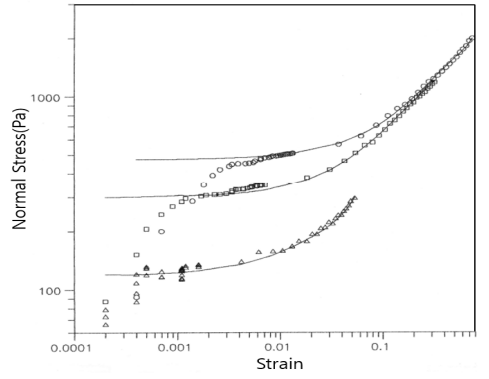

Fig. 5. Comparison of measured and calculated stresses with the geometry factor of cement paste(Initial sample height=18mm, Average strain rate: ○(0.007523s^{-1}), □(0.002760s^{-1}), △(0.000476s^{-1}), ——— calculated stresses)

stresses are exactly the same as measured normal stresses at large strain region. On the other hand, there is a limitation for the power law fluid model with the CGF factor to be compared with experimental result at very small strain region. This can be coped with dividing the curve of normal stress vs. strain into two zones such as solid and liquid behavior regions.

Under the assumption that cement paste follows a solid behavior below 0.375% of total strain from experimental results, Fig. 6. shows the comparison of measured and modeled normal stresses using elastic behavior of cement paste at very small strain region and non-Newtonian fluid behavior of cement paste at large strain region.

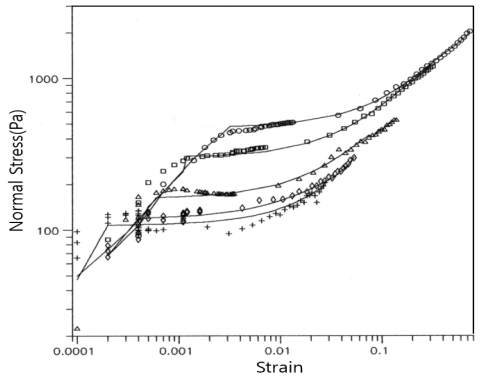

Fig. 6. Modeled normal stress divided into two zones such as linear elastic and non-Newtonian fluid((Initial sample height=18mm, Average strain rate: ○(0.000235s^{-1}), □(0.000476s^{-1}), △(0.001251s^{-1}), ◇(0.002760s^{-1}), +(0.007523s^{-1}), ——— modeled stresses)

3.2 Model of fresh cement paste as a ductile yielding solid at large strain region

A force balance analysis, used mainly in metal forming analysis, is proposed to presume the normal stress distribution under the assumption of ductile yielding material of cement paste. Constant and varying friction coefficients are considered to reflect the boundary conditions of top plate. Under the axi-symmetric compression of cement paste the element of ring type of differential thickness, dr, and height, h, at some radius, r, from the center is defined[26].

For a constant friction coefficient(μ) of Coulomb boundary condition, a force balance in the radial direction gives with higher order terms neglected:

$$2\mu\sigma_z r dr + h\sigma_\theta dr - h\sigma_r dr - hrd\sigma_r = 0 \quad (10)$$

With axi-symmetric flow, $\epsilon_\theta = \epsilon_r \; so \; \sigma_\theta = \sigma_r$, and for yielding, $\sigma_r + \sigma_z = Y$ or $d\sigma_r = -d\sigma_z$ Inserting these into Eq. (10) gives:

$$\frac{d\sigma_z}{\sigma_z} = -\frac{2\mu}{h}dr \quad (11)$$

$$\sigma_z = Ye^{(\frac{2\mu}{R}(R-r))} \quad (12)$$

where Y=2k(using the Tresca criterion) or Y= $\sqrt{3}k$ (using the von Mises criterion) and $\sigma_z = Y at \; r = R$ For the comparison of analytical and experimental results, yield strength, k, would be defined as the flat stress obtained from squeeze flow experiment. Load(L) can be calculated by integration of stress distribution of r-direction:

$$L = \int_A \sigma_z(r)dA = 2\pi Y(\frac{h}{2\mu})^2\left\{e^{(\frac{2\mu R}{h})} - \frac{2\mu R}{h} - 1\right\} \quad (13)$$

From this load, the average normal stress is calculated:

$$\sigma_{av} = \frac{1}{2}(\frac{h}{\mu R})^2 Y\left\{e^{(\frac{2\mu R}{h})} - \frac{2\mu R}{h} - 1\right\} \quad (14)$$

Eq. (14) includes the geometric parameter of the sample like the radius of sample(R) and the sample height(h) under compression. In case of experimental results, the average normal stress is obtained from the assumption of constant radius of sample like 101.6mm. As can be seen in Eq. (14), the average normal stress increases exponentially as a function of strain or squeezed sample height for various friction state at interface, in which friction state is expressed as friction coefficient. The friction coefficient at interface between top plate and sample surface seems to be varied with the proceeding of compression. In order to consider this problem, the friction coefficient is calculated as a function of strain using measured normal stress and

geometrical conditions such as radius of sample and sample height.

From Eq. (14) constant terms C_1 and C_2 are defined:

$$C_1 = \frac{1}{2}(\frac{h}{R})^2 Y \quad (15)$$

$$C_2 = \frac{2R}{h} \quad (16)$$

Eq. (14) is transformed:

$$C_1\mu^{-2}(e^{C_2\mu}) - C_2\mu - 1) - \sigma_{av} = 0 \quad (17)$$

By applying the half-interval search method, the friction coefficient is expressed by polynomial equation of strain under various experimental conditions as shown in Fig. 7. The friction coefficient increases with increasing the strain at small strain region regardless of squeezing velocity. At large squeezing velocity, the friction coefficient sustains constant value or decreases a little beyond peak value with increasing strain. The trend of friction coefficients of cement paste do not explain the behavior of friction state between interparticle since it is obtained under the concept of bulk properties related to the force balance method.

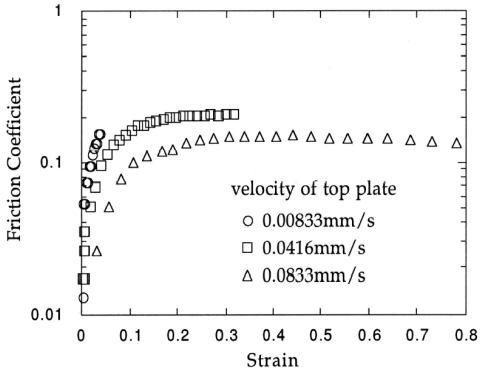

Fig. 7. Friction coefficient as a function of strain (Initial sample height=18mm, Amplitude of squeeze motion: 1mm, 5mm & 10mm)

Fig. 8. shows the comparison of experimental and model results based on the varying friction coefficient at interface. In the very small strain region between 0.0003 and 0.003, that is, the elastic solid region of the cement paste, the force balance model do not reflect the experiment result. There are still deviations at very large strain region between 0.3 and 0.8 between measured and calculated stresses because of the limitation of a theoretical result derived from the force balance method of bulk body. By comparing the force balance result with varying friction coefficient with the power-law fluid model results, cement paste seems to follow the behavior of the power-law fluid of high viscosity rather than the behavior of a ductile yielding solid under squeeze motion.

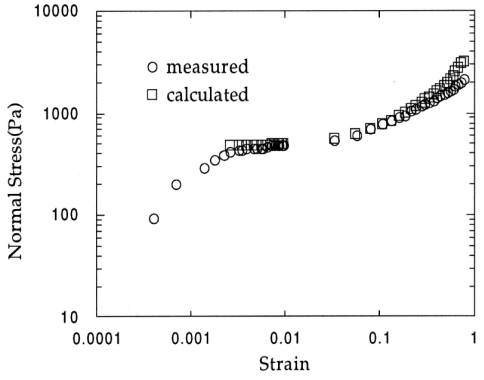

Fig. 8. Effect of varying friction coefficient on the force balance analysis(Initial sample height: 18mm, Average strain rate: 0.007523s^{-1})

4. Conclusion

From the squeeze flow experiment the relationship between normal stress and strain showed a "S" shape consisted of 3 stages. A stage I at small strain region between 0.0003 and 0.003 showed an elastic solid behavior of cement paste and stage II & III at large strain region between 0.003 and 0.8 showed a strain hardening behavior of cement paste. Rheological modelings of stage II and III were applied by using a power-law fluid model to define a liquid-like behavior and a force balance model to define a solid-like behavior of cement paste. A power-law

fluid model showed a good agreement with the experimental results at large strain region between 0.003 and 0.8 except for the elastic solid region between 0.0003 and 0.003 after reflecting the CGF to compensate the effect of ratios of a sample diameter according to various sample heights. A force balance model showed a good agreement with the experimental results only in the middle strain region between 0.003 and 0.3 except an elastic solid region between 0.0003 and 0.003 and very large strain region between 0.3 and 0.8 after reflecting the effect of friction coefficient at the interface between a top plate and sample surface. From two kinds of experimental model results, the power-law fluid model reflecting the CGF showed better agreement between measured and modeled normal stresses compared with the force balance model in the strain hardening region between 0.003 and 0.8 of cement paste under squeeze motion. It is believed that the power-law fluid model reflecting the CGF based on the experimental data can help to adjust design factors during various manufacturing processes in the future.

References

[1] F. J. Rubio-Hernandez, "Rheological Behavior of Fresh Cement Pastes," Fluids, Vol. 3, pp. 106-121, 2018.
DOI: https://doi.org/10.3390/fluids3040106

[2] M. Yang, H. M. Jennings, "Influences of Mixing Methods on the Microstructure and Rheological Behavior of Cement Paste," Advanced Cement Based Materials, Vol. 2, No. 2, pp. 70-78, Mar. 1995.
DOI: https://doi.org/10.1016/1065-7355(95)90027-6

[3] W. G. Lei, L. J. Struble, "Microstructure and Flow Behavior of Fresh Cement Paste," J. American Ceramic Society, Vol. 80, pp. 2021-2028, 1997.
DOI: https://doi.org/10.1111/j.1151-2916.1997.tb03086.x

[4] Q.Yuana, D.Zhoua, K. H. Khayat, D. Feys, C. Shi, "On the Measurement of Evolution of Structural Build-Up of Cement Paste with Time by Static Yield Stress Test vs. Small Amplitude," Cement and Concrete Research, Vol. 99, pp. 183-189, Sep. 2017.
DOI: https://doi.org/10.1016/j.cemconres.2017.05.014

[5] B. H. Min, L. Erwin, H. M. Jennings, "Hysteresis Loops of Cement Paste Measured by Oscillatory Shear Experiments," The Koran Journal of Rheology, Vol. 5, No. 2, pp. 99-108, 1993.

[6] A. W. Saak, H.M. Jennings, S.P. Shah, "The Influence of Wall Slip on Yield Stress and Viscoelastic Measurements of Cement Paste," Cement and Concrete Research, Vol. 31, pp. 205-212, 2001.
DOI: https://doi.org/10.1016/S0008-8846(00)00440-3

[7] A.Yahia, "Shear-Thickening Behavior of High-Performance Cement Grouts — Influencing Mix-Design Parameters," Cement and Concrete Research, Vol. 41, No. 3, pp. 230-235, Mar. 2011.
DOI: https://doi.org/10.1016/j.cemconres.2010.11.004

[8] J. J. Assaad, J. Harb, Y. Maalouf, "Measurement of Yield Stress of Cement Pastes using the Direct Shear Test," J. Non-Newtonian Fluid Mechanics, Vol. 214, pp. 18-27, Dec. 2014.
http://www.elsevier.com/locate/jnnfmhttps://doi.org/10.1016/J.JNNFM.2014.10.009

[9] T. Conte, M. Chaouche, "Parallel Superposition Rheology of Cement Pastes," Cement and Concrete Composites, Vol. 104, pp. 103-110, Nov. 2019.
DOI: https://doi.org/10.1016/j.cemconcomp.2019.103393

[10] B. H. Min, L. Erwin, H. M. Jennings, "Rheological Behavior of Fresh Cement Paste as Measured by Squeeze Flow," J. Materials Science, Vol. 29, pp. 1374-1381, 1994.
DOI: https://doi.org/10.1007/BF00975091

[11] Z. Toutou, N. Roussel, C. Lanos, "The Squeezing Test: A Tool to Identify Firm Cement-Based Material's Rheological Behaviour and Evaluate Their Extrusion Ability," Cement and Concrete Research, Vol. 35, No. 10, pp. 1891-1899, 2005.
DOI: https://doi.org/10.1016/j.cemconres.2004.09.007

[12] F. A. Cardoso, V. M. John, R. G. Pileggi, "Rheological Behavior of Mortars under Different Squeezing Rates," Cement and Concrete Research, Vol. 39, pp. 748-753, 2009.
DOI: http://dx.doi.org/10.1016/j.cemconres.2009.05.014

[13] F. A. Cardoso, A. L. Fujii, R. G. Pileggi, M. Chaouche, "Parallel-Plate Rotational Rheometry of Cement Paste: Influence of the Squeeze Velocity during Gap Positioning," Cement and Concrete Research, Vol. 75, pp. 66-74, Sep. 2015.
DOI: https://doi.org/10.1016/j.cemconres.2015.04.010

[14] A. Perrot, C. Lanos, P. Estellé, Y. Melinge, "Ram Extrusion Force for a Frictional Plastic Material: Model Prediction and Application to Cement Paste," Rheologica acta, Vol. 45, pp. 457-467, 2006.

[15] X. Zhou, Z. Li, M. Fan, H. Chen, "Rheology of Semi-Solid Fresh Cement Pastes and Mortars in Orifice Extrusion," Cement and Concrete Composites, Vol. 37, pp. 304-311, Mar. 2013.
DOI: https://doi.org/10.1016/j.cemconcomp.2013.01.004

[16] J. H. Kim, S. H. Kwon, S. Kawashima, H. J. Yim, "Rheology of Cement Paste under High Pressure," Cement and Concrete Research, Vol. 77, pp. 60-67, Mar. 2017.
DOI: http://lps3.doi.org.libproxy.deu.ac.kr/10.1016/j.cemconcomp.2016.11.007

[17] O. M. Reales, P. Duda, E. Silva, M. M. Paiva, R. T. Filho, "Nano-Silica Particles as Structural Buildup Agents for 3D printing with Portland Cement Pastes," Construction and Building Materials, Vol. 219, No. 20, pp. 91-100, Sep. 2019.
DOI: http://lps3.doi.org.libproxy.deu.ac.kr/10.1016/j.conbuildmat.2019.05.174

[18] M. Chen, L. Li, J. Wang, Y. Huang, S. Wang, "Rheological Parameters and Building Time of 3D printing Sulpho Aluminate Cement Paste Modified by Retarder and Diatomite," Construction and Building Materials, Vol. 234, No. 20, pp. 117-129, Feb. 2020.
DOI: http://lps3.doi.org.libproxy.deu.ac.kr/10.1016/j.conbuildmat.2019.117391

[19] M. Nehdi, M. A. Rahman, "Estimating Rheological Properties of Cement Pastes using Various Rheological Models for Different Test Geometry, Gap and Surface Friction," Cement and Concrete Research, Vol. 34, No. 11, pp. 1993-2007, Nov. 2004.
DOI: http://dx.doi.org/10.1016/j.cemconres.2004.02.020

[20] J. Peng, D. Deng, Z. Liu, Q. Yuan, T. Ye, "Rheological Models for Fresh Cement Asphalt Paste," Construction and Building Materials, Vol. 71, No. 30, pp. 254-262, Nov. 2014.
DOI: https://doi.org/10.1016/J.CONBUILDMAT.2014.08.031

[21] B. I. Choi, J. H. Kim, T. Y. Shin, "Rheological Model Selection and a General Model for Evaluating the Viscosity and Microstructure of a Highly-Concentrated Cement Suspension," Cement and Concrete Research, Vol. 123, pp. 105-111, Sep. 2019.
DOI: https://doi.org/10.1016/J.CEMCONRES.2019.05.020

[22] A. K. Jurowska, S. Grzeszczyk, M. Dziubiński, "Application of Multiple Step Change in Shear Rate Model for Determination of Thixotropic Behaviour of Cement Pastes," J. Building Engineering, Vol. 32, Nov. 2020.
DOI: https://doi.org/10.1016/j.jobe.2020.101494

[23] P. J. Leider, R. B. Bird, "Squeezing Flow between Parallel Disks. I. Theoretical Analysis," Industrial Engineering Chemical Fundamentals, Vol. 13, No. 4, pp. 336-341, 1974.
DOI: https://doi.org/10.1021/i160052a007

[24] P. Singh, V. Radhakrishnan, K. A. Narayan, "Squeezing Flow between Parallel Plates," Archive of Applied Mechanics, Vol. 60, pp. 274-281, 1990.
DOI: http://dx.doi.org/10.1007/BF00577864

[25] J. Engmann, C. Servais, A. S. Burbidge, "Squeeze Flow Theory and Applications to Rheometry: A Review," J. Non-Newtonian Fluid Mechanics, Vol. 132, pp. 1-27, 2005.
DOI: http://dx.doi.org/10.1016/j.jnnfm.2005.08.007

[26] V. S. Dixit, R. G. Narayanan, "Metal Forming: Technology and Process Modeling(Chapter 3)," pp. 147-153, McGraw Hill Education, USA, 2013.

Byeong-Hyeon Min [Regular member]

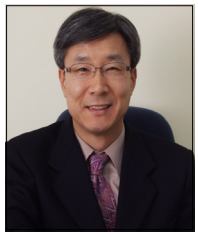

- Feb. 1985 : Pusan Nat'l Univ., Dept. of Mech. Eng., MS
- Dec. 1992 : Northwestern Univ., Dept. of Mech. Eng., PhD
- Feb. 1993 ~ Feb. 1995 : IAE, Chief Researcher
- Mar. 1995 ~ current : Dong-eui Univ., Division of Mechanical, Automobile, Robot Component Engineering, Professor

〈Research Interests〉
Rheology, Injection Molding, Optimization